

# Electronic Supporting Information: Hexanitrate complexes and hybrid double perovskites of $\text{Am}^{3+}$ and $\text{Cm}^{3+}$

Michael L. Tarlton, Suntharalingam Skanthakumar,  
Valérie Vallet, Richard E. Wilson

October 4, 2022

## List of Figures

S1	Crystals of the Am compound, representative of a typical synthesis . . . . .	3
S2	Crystals of the Cm compound, representative of a typical synthesis . . . . .	3
S3	Raman spectra of single crystals of the Am and Cm phases. The spectra were collected using an excitation line of 532 nm. The spectra are dominated by the nitrate and tetramethylammonium vibrational modes. The lack of splitting in the degenerate modes is supportive of the space group assigned . . . . .	4
S4	Raman spectra of the $[\text{Cm}(\text{NO}_3)_6\text{K}_6]^{3+}$ cluster model computed with the PBE0 functional of the density. Insets represent the displacements associated to the large intensity peaks. . . . .	5

# 1 Experimental Details

## 1.1 Synthesis

**CAUTION!**  $^{243}\text{Am}$  and  $^{248}\text{Cm}$  are alpha-emitting radionuclides with associated  $\gamma$ - and  $\beta$ -radiation from Am and its decay daughters, and neutron emissions from the spontaneous fission of Cm. These materials are manipulated in dedicated facilities for the handling of radiological materials under strict chemical and radiological controls.

Single crystals of the actinide nitrate hybrid double perovskites  $((\text{CH}_3)_4\text{N})_2\text{KLn}(\text{NO}_3)$  were crystallized by the stoichiometric (2:1:1) combination of  $(\text{CH}_3)_4\text{N}\cdot\text{NO}_3$ ,  $\text{KNO}_3$ , and  $\text{An}_{aq}$  in 4 M  $\text{HNO}_3$ . The actinide solutions were taken from ANL stocks and purified using standard ion-exchange methods[1] and assayed for concentration using liquid-scintillation counting. Typically, crystallization reactions were prepared using 1 to 5 mg of actinide. Crystal growth occurred by evaporation at room temperature or by evaporation of the reaction solution on a hot plate at 70°C. S1 S2

## 1.2 X-ray diffraction

Single crystal X-ray diffraction measurements were carried out using a Bruker Quazar microfocus source with  $\text{Mo}_{K\alpha}$  radiation and an Apex II detector. Data sets were collected at 300°K using an Oxford Cryosystems Cryostream 700 series temperature controller. Data were corrected for absorption using SADABS,[2] and subsequent structure solutions and refinements were conducted using SHELXS and SHELXL.[3] All data sets were treated with the same disorder model and corrected for extinction where appropriate. In all cases the refinements converged and provided  $R_1$  factors of between 1 and 2 %. Summaries of the crystallographic refinements are provided as CIFs including the structure factors and have been deposited with the Cambridge Crystallographic Data Center, CCDC, retrievable under accession codes 2168158 (Am) and 2168159 (Cm).

## 1.3 Vibrational Spectroscopy

Raman data were collected from single crystals using a Renishaw inVia Raman microscope with excitation wavelengths of 532 or 785 nm. Spectra were collected using circularly polarized radiation over the range of 100 to 1300  $\text{cm}^{-1}$ .

## 1.4 Quantum chemical calculations

To gain insights on the nature of the metal-nitrate chemical bonds, molecular clusters  $[\text{M}(\text{NO}_3)_3\text{K}_6]^{3+}$  were cut out of the crystal structures and the geometries were optimized with the Turbomole quantum chemistry package [4] in the gas phase with the PBE0 functional of the density [5]. Am/Eu and Cm/Gd clusters are converged to their high-spin ground states, namely sextet and septet, respectively. Relativistic effects on the lanthanide and actinide centers are accounted for small-core relativistic pseudopotentials [6, 7] and the associated segmented basis sets [8, 9], while the light atoms are described by def2-TZVP basis sets [10]. To probe the chemical character of the  $\text{M}-\text{ONO}_2$  bonds, the topology of the electron density in these bonds was analyzed by the Quantum Theory of Atoms-in-Molecules (QTAIM) [11]. Wavefunction files generated by the Gaussian 16 program [12] were processed by the AIMAll program [13].

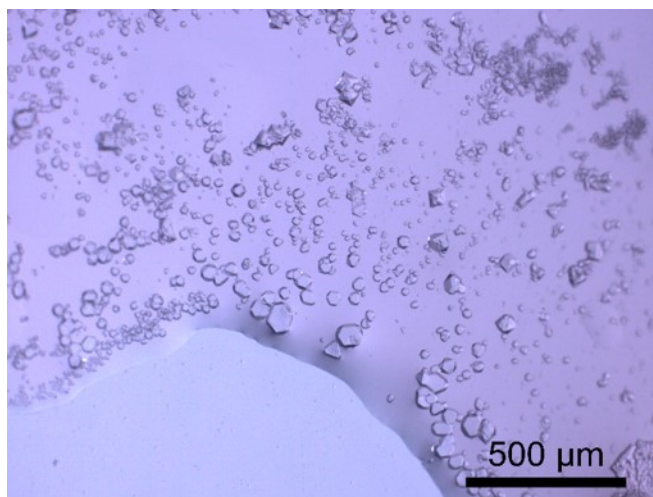


Figure S1: Crystals of the Am compound, representative of a typical synthesis

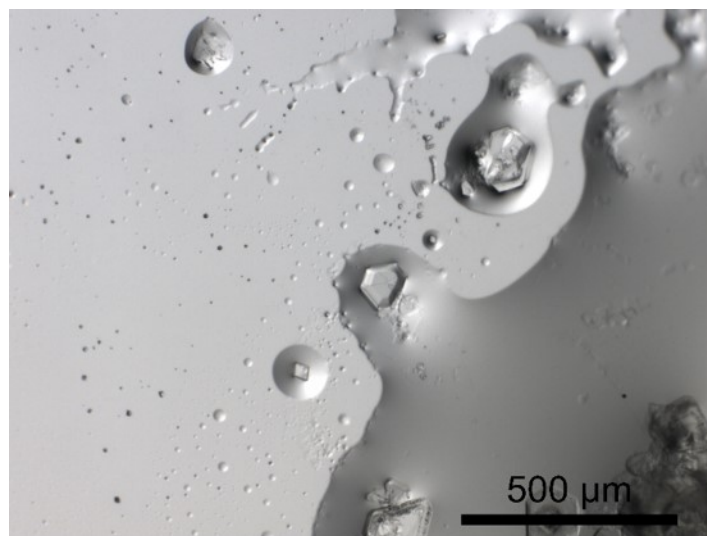


Figure S2: Crystals of the Cm compound, representative of a typical synthesis

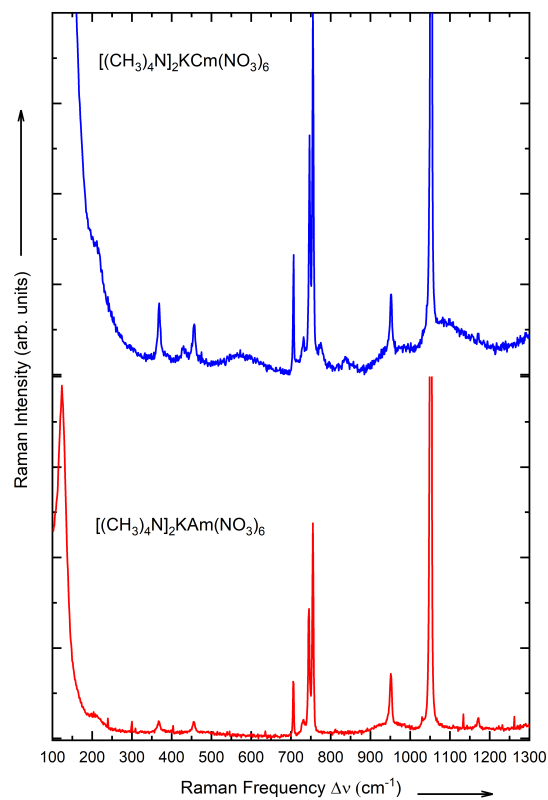


Figure S3: Raman spectra of single crystals of the Am and Cm phases. The spectra were collected using an excitation line of 532 nm. The spectra are dominated by the nitrate and tetramethylammonium vibrational modes. The lack of splitting in the degenerate modes is supportive of the space group assigned

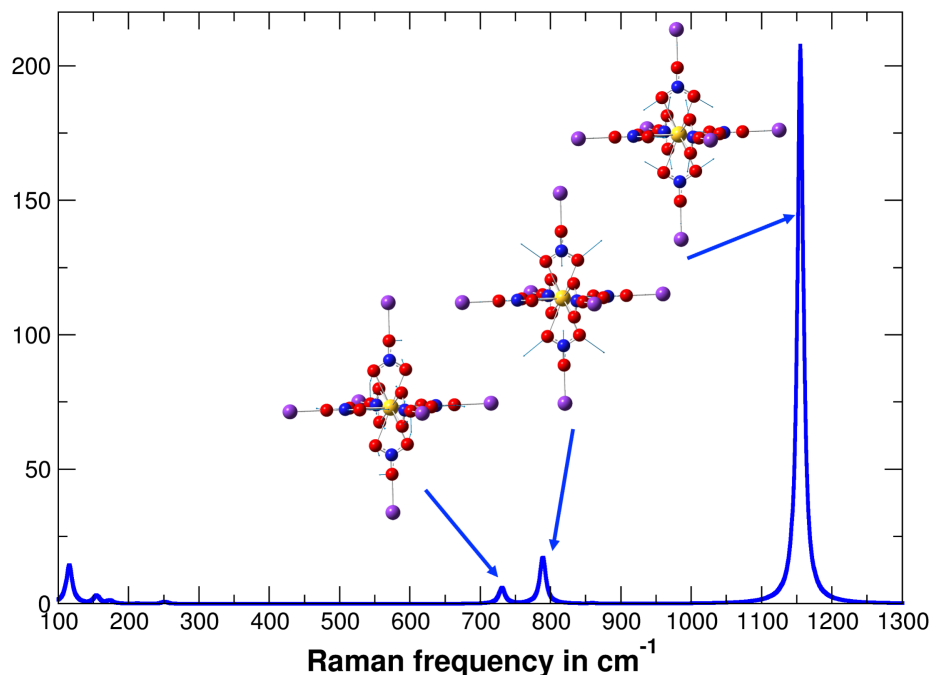


Figure S4: Raman spectra of the  $[\text{Cm}(\text{NO}_3)_6\text{K}_6]^{3+}$  cluster model computed with the PBE0 functional of the density. Insets represent the displacements associated to the large intensity peaks.

## References

- [1] E. P. Horwitz, R. Chiarizia, M. L. Dietz, H. Diamond and D. M. Nelson, *Analytica Chimica Acta*, 1993, **281**, 361–372.
- [2] G. M. Sheldrick, *Sadabs*, 1996.
- [3] G. M. Sheldrick, *Acta Crystallographica Section A: Foundations of Crystallography*, 2008, **64**, 112–122.
- [4] *TURBOMOLE V7.5.1 2021, a development of University of Karlsruhe and Forschungszentrum Karlsruhe GmbH, 1989-2007, TURBOMOLE GmbH, since 2007; available from <https://www.turbomole.org>.*
- [5] C. Adamo and V. Barone, *J. Chem. Phys.*, 1999, **110**, 6158–6170.
- [6] M. Dolg, H. Stoll and H. Preuß, *J. Chem. Phys.*, 1989, **90**, 1730–1734.
- [7] W. Küchle, M. Dolg, H. Stoll and H. Preuss, *J. Chem. Phys.*, 1994, **100**, 7535.
- [8] X. Cao and M. Dolg, *J. Mol. Struct. (Theochem)*, 2002, **581**, 139–147.
- [9] X. Cao and M. Dolg, *J. Mol. Struct. (Theochem)*, 2004, **673**, 203–209.
- [10] F. Weigend and R. Ahlrichs, *Phys. Chem. Chem. Phys.*, 2005, **7**, 3297–3305.
- [11] R. F. W. Bader, *Atoms in Molecules - A Quantum Theory*, Oxford University Press, 1994.

- [12] M. J. Frisch, G. W. Trucks, H. B. Schlegel, G. E. Scuseria, M. A. Robb, J. R. Cheeseman, G. Scalmani, V. Barone, G. A. Petersson, H. Nakatsuji, X. Li, M. Caricato, A. V. Marenich, J. Bloino, B. G. Janesko, R. Gomperts, B. Mennucci, H. P. Hratchian, J. V. Ortiz, A. F. Izmaylov, J. L. Sonnenberg, D. Williams-Young, F. Ding, F. Lipparini, F. Egidi, J. Goings, B. Peng, A. Petrone, T. Henderson, D. Ranasinghe, V. G. Zakrzewski, J. Gao, N. Rega, G. Zheng, W. Liang, M. Hada, M. Ehara, K. Toyota, R. Fukuda, J. Hasegawa, M. Ishida, T. Nakajima, Y. Honda, O. Kitao, H. Nakai, T. Vreven, K. Throssell, J. A. Montgomery, Jr., J. E. Peralta, F. Ogliaro, M. J. Bearpark, J. J. Heyd, E. N. Brothers, K. N. Kudin, V. N. Staroverov, T. A. Keith, R. Kobayashi, J. Normand, K. Raghavachari, A. P. Rendell, J. C. Burant, S. S. Iyengar, J. Tomasi, M. Cossi, J. M. Millam, M. Klene, C. Adamo, R. Cammi, J. W. Ochterski, R. L. Martin, K. Morokuma, O. Farkas, J. B. Foresman and D. J. Fox, *Gaussian~16 Revision C.01*, 2016, Gaussian Inc. Wallingford CT.
- [13] T. A. Keith, *AIMAll (version 19.10.12)*, Todd A. Keith, *TK Gristmill Software: Overland Park KS, 2019*, <http://aim.tkgristmill.com>.